INFLUENCE OF SAWDUST, SUGARCANE BAGASSE AND THEIR SYNERGY ON THE MORPHOLOGICAL, THERMAL AND MECHANICAL PROPERTIES OF THE PHBH MATRIX

S. T. SIKHOSANA,[*] N. J. MALEBO,[*] T. G. MOFOKENG,[**] M. P. MOTLOUNG[***] and M. J. MOCHANE[***]

[*]*Department of Life Sciences, Central University of Technology, Free State, Bloemfontein, South Africa*
[**]*Centre for Nanostructures and Advanced Materials, DSI-CSIR Nanotechnology Innovation Centre, Council for Scientific and Industrial Research, Pretoria 0001, South Africa*
[***]*Department of Chemistry, College of Science, Engineering, and Technology, University of South Africa, Roodepoort, Johannesburg, South Africa*
✉ *Corresponding author: M. J. Mochane, mochane.jonas@gmail.com*

Received August 8, 2025

The accumulation of agricultural waste is a serious concern worldwide. The primary goal of this paper is to examine the microstructure, thermal, mechanical and rheological properties of sugarcane bagasse and sawdust reinforced hybrid composites. Poly(3-hydoxybutyrate-co-3-hydroxyhexanoate) was employed as a polymer matrix phase, and the composites were prepared by melt extrusion at 178.8 rpm using a twin-screw extruder. The morphological features show poor interfacial adhesion between the polymer matrix and sugarcane bagasse, but sawdust shows better dispersion in the matrix. The hybrid composite comprising halloysite clay showed higher thermal stability and viscosity than all other composites. All composites showed better stiffness than the neat matrix, irrespectively of the type of reinforcing filler. The results showed that the combination of sugarcane bagasse, sawdust and halloysite clay is useful for improving the thermal stability and stiffness of the polymer matrix. This enhancement is particularly advantageous for advanced applications, such as smart packaging solutions and electronics, where the interplay of thermal properties and rigidity is important.

Keywords: sugarcane bagasse, sawdust, PHBH, hybrid composite, agricultural waste

INTRODUCTION

Selecting appropriate materials for design and manufacturing is an essential component of engineering. This process facilitates the evaluation of the physical and mechanical properties of materials, ultimately leading to improved product performance and enhanced customer satisfaction.[1] Natural fibres possess unique characteristics that set them apart from other classes of materials, particularly in terms of their physical, chemical, thermal, mechanical, and electrical properties.[2] These fibres have diameters ranging from a few micrometres to tens of micrometres and lengths ranging from millimetres to centimetres, resulting in moderate to high aspect ratios.[3] They also offer tensile strengths between 80–1500 MPa and Young's moduli in the range of 3–80 GPa, depending on the type of fibre and its treatment.[4,5] Furthermore, natural fibres offer good thermal insulation, biodegradability, and low density (1.2–1.6 g/cm^3), making them attractive for lightweight materials.[1] However, factors such as fibre type, fibre-matrix adhesion, surface treatment, fibre content, and processing conditions strongly influence their properties. Moisture sensitivity and thermal stability, which is usually limited to temperatures below 200–250 °C, are significant challenges.[4] However, these shortfalls can be addressed through various surface treatments (mechanical, physical, chemical, biological, *etc*.), which can be further enhanced via hybridization with other fibres and/or compatible materials.[2,6,7] Fibre properties collectively determine their effectiveness as fillers or reinforcements in natural fibre composites (NFCs). These characteristics ultimately shape their performance and define their potential applications across various industries and markets. Thus, they are currently explored in fibre polymer composites, where they are embedded in various polymer matrices for advanced sustainable applications.[7,8,9]

Among the various natural reinforcements studied, sawdust (SD) and sugarcane bagasse (SB) have emerged as promising candidates due to their abundance, renewability, and favourable mechanical and

thermal properties.[10,11] These lignocellulosic fibres primarily consist of cellulose, hemicelluloses, and lignin, each contributing to their performance in polymer matrices. Cellulose provides structural rigidity and high tensile strength, while lignin offers thermal stability and hydrophobic properties, which improve adhesion in non-polar systems.[12] The potential of SD and SB as reinforcement is closely associated with their physicochemical structure, including a high aspect ratio and surface area. Sawdust with higher lignin content can enhance thermal stability and promote matrix compatibility through lignin–polymer interactions.[13] Sugarcane bagasse, rich in cellulose, significantly contributes to mechanical reinforcement and thermal resistance.[10] Moreover, both fibres possess abundant hydroxyl groups that facilitate interfacial bonding with polar polymer matrices through hydrogen bonding. When modified, these functional groups are capable of covalent interactions, such as esterification. Such interactions promote enhanced stress transfer and reduce fibre-matrix debonding. Additionally, the fibrous morphology of these materials enables effective load distribution within the matrix, thereby improving the mechanical integrity of the composite.[12] Their distinct yet complementary properties make them ideal candidates for hybrid composites that deliver enhanced mechanical strength, improved thermal resistance, and overall performance optimisation in sustainable material applications.

In our previous study on polybutylene succinate (PBS)-based composites incorporating sawdust (SD), sugarcane bagasse (SB), and halloysite nanotubes (HS),[14] we observed significant enhancements in thermal stability and mechanical stiffness, attributed to improved compatibility between the fillers and the PBS matrix. The inclusion of SD and SB increased the complex viscosity and stiffness of PBS, while further enhancements were achieved with the addition of low concentrations of HS and expandable graphite (EG), resulting from better filler-matrix interactions. Differential scanning calorimetry indicated that the filled composites demonstrated higher crystallisation temperatures, with EG exhibiting superior nucleation efficiency compared to HS. Dynamic mechanical analysis confirmed an increase in storage modulus across varying temperatures; however, the thermal stability was slightly compromised by the presence of fillers. Despite these enhancements, poor interfacial adhesion between the PBS and natural fibres was evident, resulting in issues such as voids, reduced toughness, elongation at break, and reduced impact strength. The authors concluded that low levels of HS and EG could effectively improve the rheological, thermal, and mechanical properties of PBS/SD/SB hybrid composites, indicating potential for sustainable, rigid biodegradable materials such as packaging solutions. Building on our previous findings with PBS matrices, this study investigates the influence of SD and SB fillers, both individually and in hybrid combinations with HS, on the rheological, thermal, and mechanical properties of polyhydroxybutyrate-co-hydroxyvalerate (PHBH) composites prepared through melt extrusion. Like PBS, PHBH is a polyester; however, its bio-based and relatively hydrophilic nature distinguishes it from PBS and may enhance interfacial interactions with lignocellulosic fibres and halloysite nanotubes, offering an underexplored pathway for achieving synergistic reinforcement in sustainable biocomposites.

EXPERIMENTAL

Materials

The poly(3-hydoxybutyrate-co-3-hydroxyhexanoate) (PHBH) polymer grade Green Planet™ X131A was purchased from Kaneka Corporation (KITA-KU Osaka, Japan) in the form of pellets. It has a melt flow index of 3.0 g/10 min, and a density of 1.25 g/cm³. Sugarcane bagasse (SB), of 4 mm length, was obtained from Tongaat hullet, Kwazulu Natal (South Africa). Ground sawdust (SD) was sourced from a timber processing plant in Bloemfontein, Free State (South Africa) and it had a size ranging between 10 μm to 30 μm. Halloysite nanoclay powder (HS), beige coloured with a formula weight of 294.19 g/mol and a pore size of 1.26-1.34 mL/mol, was purchased from Sigma-Aldrich, South Africa. Its particles have a diameter of 30-70 nm and a length of 1-3 microns.

Preparation of the investigated samples

SB fibres were prepared following the method reported in our previous research.[14] A screw speed of 178.8 rpm was chosen for melt extrusion to optimize filler dispersion and reduce thermal degradation of the bio-based components, based on preliminary trials. Prior to melt extrusion, PHBH, SB, SD and HS were dried at 60 °C in a vacuum oven for 12 hours. The compositions of the samples are shown in Table 1. The neat PHBH, binary, and hybrid composites were extruded in a TE-30 co-rotating twin-screw extruder (Nanjing Only Extrusion Machinery Co., Ltd.) with the temperatures of the heating zones from the hopper to the die set from 120 to 160

°C. The extrusion speed and feed rate were set at 178.8 rpm and 4.4 kg/h, respectively. The extrudates were then quenched in water, pelletized, and dried in an oven at 60 °C for 24 hours. These dried pellets were injection moulded into various test specimens using an injection moulding machine (ENGEL E-Mac50). The injection moulding heating zones were set at 36, 120, 140, 150, and 160 °C. The clamping force, metering, specific back pressure, injection pressure, and injection speed were set at 500 kN, 29 mm, 100 bar, 550 bar, and 100 m/s, respectively. The test specimens were cooled to 22 °C and stored in a Ziplock bag.

Table 1
Composition of the investigated samples

Sample ID	Composition (wt%)
PHBH	100
PHBH/SB	90/10
PHBH/SD	90/10
PHBH/SB/SD	90/5/5
PHBH/SB/SD/HS	87.3/4.85/4.85/3

Characterizations of the investigated samples

Scanning electron microscopy (SEM)

The morphology of cryo-fractured composite samples was investigated using a JSM-7800F Extreme-Resolution Analytical Field Emission Scanning Electron Microscope (JEOL Ltd, Akishima City, Tokyo, Japan), which was operated at an accelerating voltage of 5.0 kV. The samples were mounted on 10 mm Cambridge pin-type aluminium stubs using epoxy glue for precise imaging. The high-resolution capabilities of the JSM-7800F allowed for detailed qualitative analysis of the surface morphology and texture of the materials.

Differential scanning calorimetry (DSC)

DSC tests were performed using a Perkin Elmer DSC7 instrument (Norwalk, Connecticut, USA). Samples weighing ≈ 6 mg were sealed in aluminium pans and heated under nitrogen flow of 20 mL/min from -35 to 160 °C, at a heating rate of 10 °C/min, and kept at this temperature for 1 minute to eliminate the thermal history, cooled to -35 °C at the same rate, and reheated under the same conditions. The melting enthalpies and temperatures were determined from the second heating curves.

Thermogravimetric analysis (TGA)

The thermogravimetric analysis (TGA) was done in a Perkin Elmer Pyris-1 thermogravimetric analyzer (model Q500, TA Instruments, New Castle, DE, USA). The specimens with a size of ≈ 8 mg were heated from 25 to 800 ℃, at a heating rate of 10 ℃ min^{-1} under inert nitrogen.

Dynamic rheological properties

The dynamic rheological properties were examined under the atmospheric conditions with a temperature of 190 ℃ by utilizing a Physica MCR501 (Anton Paar, Austria) rheometer in a 25 mm diameter parallel plate configuration. The strain amplitude of 1% was determined with preliminary experiments and the zero gap was set at 1.15 mm for all the tests.

Dynamic mechanical analysis (DMA)

The dynamic mechanical properties of the neat PHBH and its hybrid composites were analyzed by Perkin Elmer Diamond DMA (USA) in dual cantilever-bending mode. Samples with a thickness of 1 mm were heated from -60 ℃ to 80 ℃ at a rate of 5 ℃ min^{-1} at an oscillating frequency of 1 Hz. The length of the samples was 30 mm and the width of 10 mm.

Tensile test

Tensile testing was carried out on the injection-moulded, dog-bone-shaped specimens using an Instron 5966 tester (Instron Engineering Corporation, USA, ASTM 638D). The tensile tester is equipped with a 10 kN load cell, and the tests were conducted at a constant strain rate of 50 mm/min and a temperature of 25 °C. The results are an average of six tests per sample, along with standard deviations.

Impact resilience (Charpy impact test)

The injection moulded specimens of the different formulations, with dimensions of approximately 80 mm × 10 mm × 4 mm (L×W×B), were subjected to a Charpy impact test in accordance with the instrumented ISO179-1-2010 standard to evaluate their resistance to breakage by flexural shock. The specimens were notched on one side with a 0.25 mm notch root radius at a depth of 2 mm using a CEAST Automatic Notchvis Plus (Instron,

Noorwood, MA, USA). The notched Charpy impact strength was measured at 25 °C using a fully automated CEAST Pendulum Resil Impactor II. The drop velocity was 3.7 m/s, resulting in a hammer energy of 14 J. The reported results represent the average of at least six tests per sample.

RESULTS AND DISCUSSION

Scanning electron microscopy

Figure 1 shows the SEM images of the fractured surfaces of the composites. In Figure 1a, there are voids due to SB fibre pull-outs and SB gaps in the PHBH matrix. This indicates poor compatibility between the hydrophobic PHBH matrix and hydrophilic SB. Larger and elongated SB fibres clustered together, creating regions of poor distribution. In Figure 1b, there are vacant spaces of SD that are randomly distributed within the PHBH matrix. Voids are also visible, suggesting poor compatibility between SD and the PHBH matrix. The fine SD particles in Figure 1b show better dispersibility and distribution in PHBH than SB. The morphology of the PHBH/SB/SD composite in Figure 1c is a combination of the morphologies from Figure 1(a,b), but voids are present, indicating poor interfacial adhesion between the fillers and the PHBH matrix. The morphology of the PHBH/SB/SD/HS composite is finer than that of the other composites. This can be attributed partly to its lower total biomass content of 4.85 wt% for the mixed SD and SB, compared to 10 wt% in the binary PHBH/SB and PHBH/SD composites. The reduced biomass content minimises agglomeration and enhances the distribution within the matrix. Theys *et al.*[15] reported a compatibilizing effect of montmorillonite (MMT) in a hybrid polybutylene succinate (PBS)/maize stalk fiber (MSF)/MMT bio-composite. However, there is an interfacial gap between the long SB and PHBH matrix in Figure 1d, suggesting poor compatibility between SB and the matrix, despite the presence of HS. The surface treatments of the fibres or modifying the halloysite, as through surface functionalization or intercalation with specific compounds, could enhance interfacial adhesion between the constituents of the composite and optimize performance.[16,17]

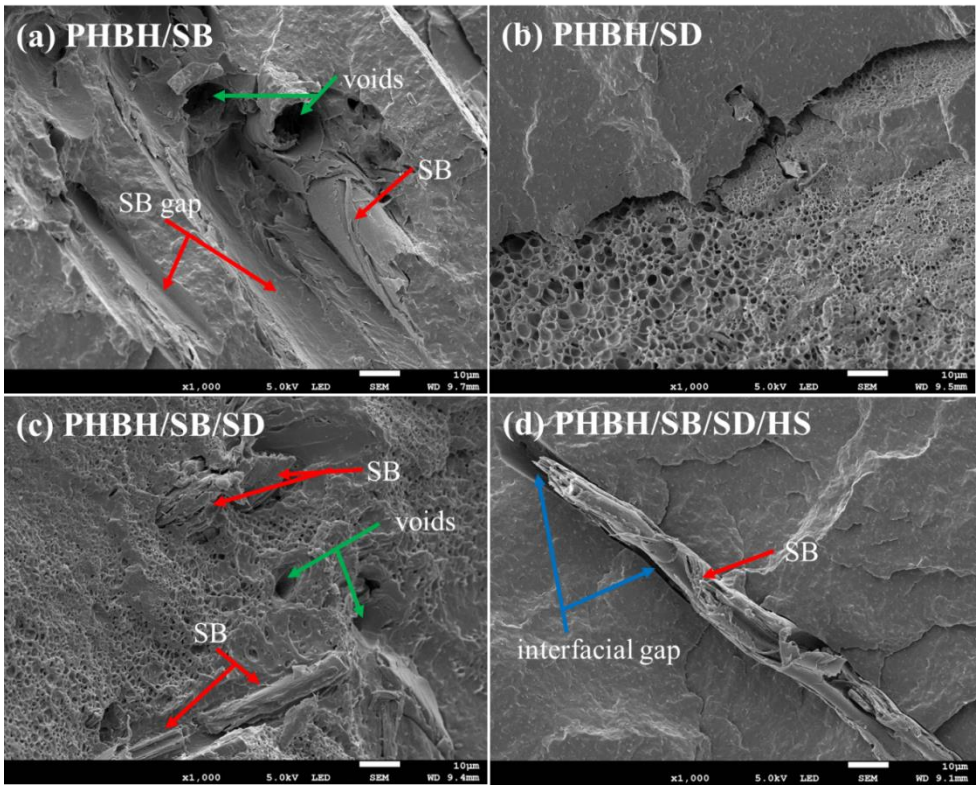

Figure 1: SEM micrographs of fractured surfaces of (a,b) binary composites and of (c,d) hybrid composites

Differential scanning calorimetry (DSC)

Displayed in Figure 2 are the second melting and first cooling curves of neat PHBH, binary and hybrid composites. Neat PHBH in Figure 2a shows two melting peaks, T_{m1} and T_{m2} at 134 and 146.1 °C, respectively. The T_{m1} has a relatively lower intensity than T_{m2}. The double melting phenomenon

for PHBH has been reported in literature.[18] Hu *et al.*[18] attributed the lower and higher melting peaks to the melting of crystals formed during the primary crystallization, and the melting of crystals formed by recrystallization during the heating process, respectively. The lower and higher melting peak positions do not change in the presence of the fillers (SB, SD, HS), suggesting that the lamellae thickness of PHBH crystals is not altered in the binary and hybrid composites. Neat PHBH has a crystallization temperature (T_c) of 96.7 °C. The introduction of fillers for binary and hybrid composites lowers the T_c, so that the composites have a T_c at about 87 °C. The presence of fillers in the composites disrupts the mobility of PHBH chains, making it difficult for the chains to pack orderly to form crystals, hence crystallization is delayed. The standard melting enthalpy of a 100% crystalline PHBH polymer (ΔH^0_m) is equal to 146 J/g.[19] The ΔH^{norm}_m is obtained by dividing the DSC measured melting enthalpy ($\Delta \mathbf{H_m}$) of PHBH in the samples with the weight fraction of PHBH. The degree of crystallinity (X_c) of the material was determined according to the following equation:

$$X_c = (\Delta H^{norm}_m / \Delta H^0_m) \text{ X } 100 \qquad (1)$$

In the binary composites, the addition of SB slightly reduces normalized melting enthalpy (ΔH^{norm}_m) and the crystallinity (X_c) of PHBH, whereas introduction of SD increases ΔH^{norm}_m and X_c, as seen in Table 2. Earlier, the SEM results in Figure 1 showed poorly distributed clusters of SB in the PHBH matrix due to poor compatibility between the constituents of the composites. The inadequate compatibility promotes the formation of imperfect crystals, hence a slightly lower ΔH^{norm}_m and X_c for the PHBH/SB composite. High ΔH^{norm}_m and X_c for the PHBH/SD composite are linked to better dispersion of SD particles due to their larger surface area, which promote better alignment of PHBH chains. The ΔH^{norm}_m and X_c of the PHBH/SB/SD composite despite the presence of fillers are equal to those of neat PHBH. The fillers in the PHBH/SB/SD composite have two opposing effects on ΔH^{norm}_m and X_c. To be precise, SB reduces ΔH^{norm}_m and X_c, whereas SD promotes the increase of ΔH^{norm}_m and X_c. The net effect is ΔH^{norm}_m and X_c that are equal to those of neat PHBH. The PHBH/SB/SD/HS composite has ΔH^{norm}_m and X_c that are slightly higher than those of the PHBH/SB/SD composite due to the influence of HS.

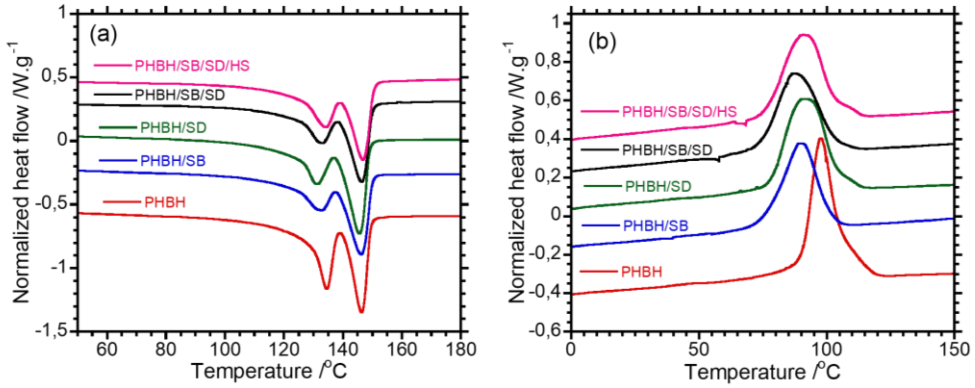

Figure 2: DSC (a) second heating and (b) cooling curves of neat PHBH, binary and hybrid composites

Table 2
Melting and crystallization parameters obtained from DSC

Samples	T_{m1} (°C)	T_{m2} (°C)	T_c (°C)	ΔH_m (J.g^{-1})	ΔH^{norm}_m (J.g^{-1})	X_c (%)
PHBH	134.1	146.06	96.7	63.7	63.7	43.6
PHBH/SB	131.97	146.06	88.57	53.73	59.7	40.9
PHBH/SD	130.89	145.33	87.85	62.55	69.5	47.6
PHBH/SB/SD	131.97	145.69	86.11	57.51	63.9	43.8
PHBH/SB/SD/HS	133.78	146.42	88.05	57.71	66.1	45.3

Thermogravimetric analysis (TGA)

The TGA curves and $T_{5\%}$, $T_{50\%}$ and T_{max} values of the samples are shown in Figure 3 and Table 3. The $T_{5\%}$, $T_{50\%}$ and T_{max} values of neat PHBH are lower, indicating that the neat polymer has lower thermal stability than the composites. The thermal stability of PHBH is enhanced by incorporating

either SB or SD. SD and SB are lignocellulosic materials composed of cellulose, hemicelluloses and lignin. The lignin of the fillers acts as a stabilizer, which reduces the degradation rate of PHBH in the composites; hence, high thermal stability is achieved.

There are disagreements in the literature regarding the influence of cellulose based materials on the thermal stability of polymer matices.[20,21] Masanabo *et al.*[20] reported a decrease in the overall thermal stability of poly(butylene succinate-co-adipate)/poly(3-hydroxybutyrate-co-3-hydoxyvalerate) blends when cowpea lignocellulosic side stream/fibres were incorporated. In contrast, Valente *et al.*[21] reported that high contents of cellulose fibres (40 wt%) enhance the maximum thermal degradation temperature of poly(hydroxybutyrate) (PHB) from 236 °C to over 280 °C. The researchers suggested that the increase in thermal stability proves that there is some degree of interfacial adhesion between PHB and the fibers. The SD shows better improvement of thermal stability for the PHBH/SD composite than PHBH/SB composite. Earlier, the SEM results showed better dispersion of SD than SB in the PHBH matrix for binary composites due to its smaller size. The smaller SD particles interacted better with the PHBH matrix promoting better heat dissipation and high thermal stability. The simultaneous incorporation of SB and SD to PHBH has a synergistic effect on the thermal stability. The PHBH/SB/SD/HS composite shows the highest thermal stability among the composites, as observed from the $T_{5\%}$, $T_{50\%}$ and T_{max} values. The presence of HS in the PHBH/SB/SD/HS composite hinders the diffusion of volatile decomposition products from the composite by stabilizing the matrix; hence, a relatively higher thermal stability is achieved.

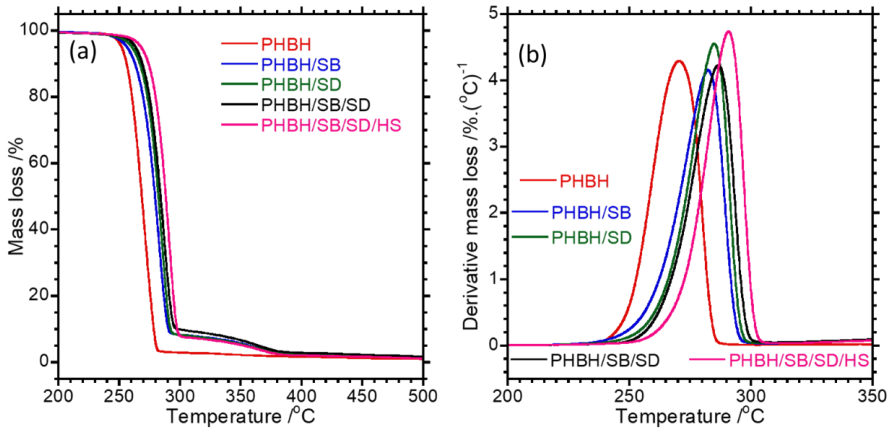

Figure 3: (a) Thermogravimetric and (b) derivative (dTGA) curves of neat PHBH, binary and hybrid composites

Table 3
Degradation parameters obtained from thermogravimetry

Samples	$T_{5\%}$ (°C)	$T_{50\%}$ (°C)	T_{max} (°C)
PHBH	251.8	268.8	270.4
PHBH/SB	256.5	279.6	281.1
PHBH/SD	260.7	282.3	284.6
PHBH/SB/SD	263.5	284.2	286.7
PHBH/SB/SD/HS	268.1	288.4	290.8

Rheological studies

Rheological studies are important in polymer processing because they provide insights regarding the processability of polymer composites. The complex viscosity (η*) curves of neat PHBH, binary and hybrid composites as a function of angular frequency (ω) are illustrated in Figure 4. The amplitude was set to 1%, following the preliminary amplitude sweep tests conducted to determine the linear viscoelastic region of the samples. Neat PHBH exhibits lower η* due to its molecular structure, which lacks significant covalent crosslinks, resulting in fewer entanglements and constrictions on the chain movement. The polymer chains are mobile, permitting ease of flow when subjected to shear pressures or elevated temperatures. In Figure 5, the composites have higher η* than neat PHBH. The addition of stiff materials into the PHBH matrix hinders the mobility of the polymer chains, thus

affecting the viscous behaviour by causing an increase in η*.[22] The increase in η* after addition of fillers suggests enhanced resistance to flow and may indicate improved melt strength of the composite melt. The η*of the composites in Figure 4 increases in the following order: PHBH/SB < PHBH/SD < PHBH/SB/SD < PHBH/SD/SB/HS. The higher η* of the PHBH/SD composite in comparison with the PHBH/SB composite is linked to the different dispersion states of the fillers in the composites, as seen in Figure 1. The fine SD particles dispersed better in the PHBH matrix than the longer SB fibres that formed clusters. The uniformly dispersed SD particles offered a relatively greater restriction on PHBH chain mobility than SB. Consequently, a relatively higher η* and elasticity of PHBH/SD were realised.

The viscous behaviour of a polymer material is not solely dependent on the dispersion state of the filler; it can also be influenced by the shape, size, and interactions of filler particles.[23] In hybrid composites, the combination of sugarcane bagasse and sawdust exhibits a higher η* than single-fibre composites despite containing equal filler loadings. The combination of 5 wt% SB and 5 wt% SD in PHBH/SB/SD composite forms a percolation network, compared to the individual fillers at 10 wt% loading. The network contributes to enhanced η*. A better η* PHBH/SD/SB/HS composite is attributed to HS intercalation within SB and SD, preventing the agglomeration of sawdust and forming a dense hybrid network in the process. A dense network promotes enhanced η* due to entanglements and/or interactions.[24]

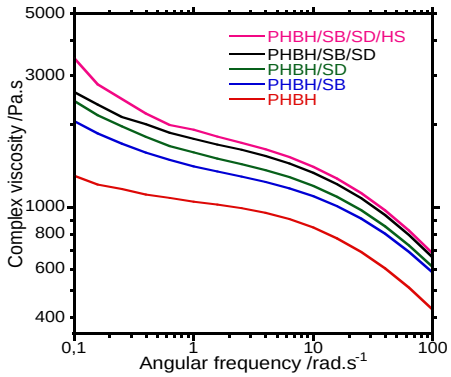

Figure 4: Viscosity curves of neat PHBH, binary and hybrid composites at 190 °C

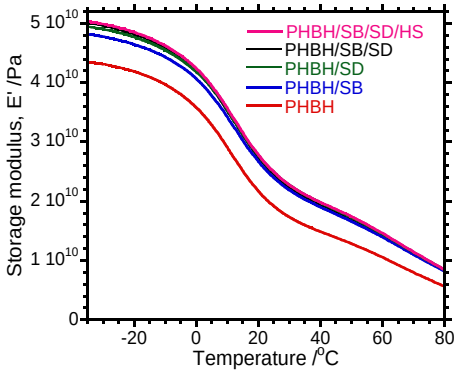

Figure 5: Temperature dependence of storage modulus of neat PHBH, binary and hybrid composites

Dynamic mechanical analysis

The storage modulus (E') of neat PHBH and the composites is shown in Figure 5(a). Neat PHBH has a lower E' than the composites for the tested temperatures. Overall, the composites have better stiffness than neat PHBH due to the presence of fillers that restrict the mobility of polymer chains. The PHBH/SD composite has higher stiffness than the PHBH/SB composite, and this can be linked to different morphologies of the composites. Earlier, the finer SD particles showed superior distribution in PHBH to the SB fibres that formed clusters in the matrix (Fig. 1). In a relatively better dispersed system, such as PHBH/SD, the SD particles promoted effective immobilization of the polymer chains, hence better reinforcement is achieved. The higher X_c of the PHBH/SD composite than that of PHBH/SB composite may have also contributed to its relatively higher stiffness. The stiffness of PHBH is enhanced by the addition of the combination of SD and SB due to their synergistic effect. The PHBH/SB/SD/HS composite exhibits better stiffness amongst all the other composites. This behaviour is ascribed to higher stiffness HS nanotubes due to their rigidity and their promotion of better intimate contact between the SD and PHBH. The storage modulus follows a similar trend of the flow curves.

Mechanical properties of the investigated samples

The mechanical properties of the samples are shown in Figure 6 and Table 4. The mechanical properties of polymer composites are influenced by several factors, including dispersion, interfacial adhesion, geometry, and the synergistic interactions among the components in the formulation.[25] In this study, two primary contributors to mechanical properties were identified: the degree of dispersion and the stiffness of individual components, with dispersion being the dominant factor. In binary

systems in Figure 6a, it was observed that SD composites exhibited a slightly higher average tensile modulus compared to SB composites, though with greater variability (larger error bars) potentially because of dispersion inconsistencies. SEM analysis confirmed that SD achieved better dispersion within the PHBH matrix than SB. This improved dispersion facilitated more efficient stress transfer between the matrix and the filler, highlighting the importance of uniform distribution. Additionally, the intrinsic stiffness of the individual fillers significantly influenced mechanical properties. In contrast, hybrid systems exhibited poor filler dispersion, resulting in a lack of synergy among the components. Consequently, no enhancement in mechanical properties was observed. The lack of synergy may be due to the orientation and incompatibility of the fillers. In particular, the combination of fine powders and longitudinal fibres appeared to impede effective interaction within the matrix, which is supported by SEM images. This anti-synergy led to diminished mechanical performance, contrary to expectations that the hybrid system would yield superior tensile strength through collaborative interactions among the fillers. Furthermore, the anticipated increase in tensile modulus, driven by the addition of high-aspect-ratio fillers like HS, was not achieved. This shortfall was attributed to a lack of affinity between the fillers, which limited stress transfer and reduced the tensile modulus. None of the fillers were effectively adhered to halloysite clay, further diminishing their potential to enhance mechanical properties. In summary, the findings emphasize the critical roles of dispersion and compatibility in influencing the mechanical properties of composite materials. The lack of collaboration among the fillers, combined with poor dispersion in the hybrid systems, negated any potential benefits from their inclusion, highlighting the need for optimized filler selection and dispersion strategies in future studies.

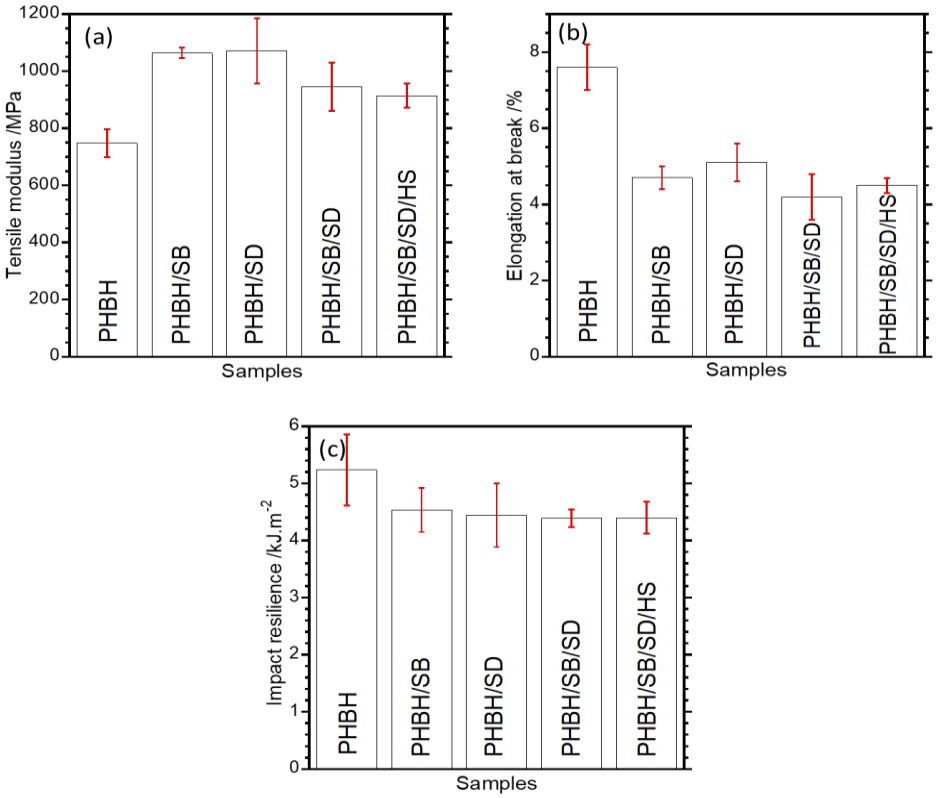

Figure 6: (a) Tensile modulus, (b) elongation at break, and (c) impact resilience of neat PHBH, binary and hybrid composites

Table 4
Tensile and impact data of neat PHBH, binary and hybrid composites

Sample	Tensile modulus (MPa)	Elongation at break (%)	Impact resilience ($kJ.m^{-2}$)
PHBH	748.2 ± 49.4	7.6 ± 0.6	5.2 ± 0.6
PHBH/SB	1063.8 ± 18.5	4.7 ± 0.3	4.5 ± 0.4
PHBH/SD	1071± 113	5.1 ± 0.5	4.5 ± 0.5
PHBH/SB/SD	945 ± 84.5	4.2 ± 0.6	4.4 ± 0.2
PHBH/SB/SD/HS	914.5 ± 42.1	4.5 ± 0.2	4.4 ± 0.3

In Figure 6(b,c), neat PHBH polymer exhibits higher elongation at break and impact resilience than the binary and hybrid composites. The addition of stiff reinforcements, such as SD, SB, and HS introduces rigidity to the polymer matrix, which restricts chain mobility. This reduction in chain mobility reduces ductility of the polymer matrix, making it more brittle under mechanical stress.

The compatibility between the polymer matrix and the added fillers is a critical factor that influences the mechanical properties of the composites. Poor interfacial adhesion between the hydrophobic PHBH polymer and the hydrophilic fibres, as seen in Figure 1, promotes the formation of cracks, voids, and weak interfacial regions within the composite. These defects act as stress concentrators or crack initiators, significantly diminishing the ability of the material to absorb and dissipate energy upon impact. Consequently, the composites show reduced impact resistance compared to the neat polymer.[6,22,26] Incorporating compatibilization strategies could mitigate these defects, improve fibre-matrix bonding, and enhance both tensile and impact performance of the composites.

CONCLUSION

The investigation of the morphology suggested poor interfacial compatibility in the hybrid composites because of the hydrophobicity of PHBH and the hydrophilic nature of SB and SD, as evidenced by voids and pull-outs in SEM images, but the PHBH/SD composite showed better dispersion of the filler. The differences in morphologies account for the variations in composite performance. Compared to pristine PHBH, the binary and hybrid composites demonstrated superior stiffness, viscosity and storage modulus. The thermal stability of PHBH was enhanced with the addition of SB and SD, but the mixture of the fillers showed a synergistic effect on thermal stability. However, the presence of HS in the PHBH/SB/SD/HS achieved higher thermal stability of the composite due to the barrier effect of HS. The addition of fillers resulted in a reduction in elongation at break and impact resilience of PHBH, although the elongation of the composites remained within a similar range. The reduction in mechanical properties provides evidence of high interfacial tension between PHBH and either SB or SD in the hybrid composites. In future work, maleic anhydride grafted poly(3-hydroxybutyrate-co-3-hydroxyhexanoate) (PHBH-g-MA) will be produced to investigate its effectiveness as a compatibiliser at various loadings for PHBV/SB, PHBH/SD, PHBH/SB/SD, and PHBH/SB/SD/HS composites prepared through melt extrusion.

ACKNOWLEDGENTS: This work was supported by the National Research Foundation of South Africa, Grant/Award Numbers 127278 and 129347.

REFERENCES

[1] Y. G. Girijappa Thyavihalli, S. Mavinkere Rangappa, J. Parameswaranpillai and S. Siengchin, *Front. Mater*., **6**, 1 (2019), https://doi.org/10.3389/fmats.2019.00226

[2] R. V. Patel, A. Yadav and J. Winczek, *Appl. Sci*., **13**, 5126 (2023), https://doi.org/10.3390/app13085126

[3] S.-Y. Fu, B. Lauke, Y.-W. Mai and C.-Y. Yue, "Science and Engineering of Short Fibre Reinforced Polymer Composites", Oxford, Woodhead Publishing, 2009, p. 1. https://doi.org/10.1533/9781845696498.1

[4] M. A. Musthaq, H. N. Dhakal, Z. Zhang, A. Barouni and R. Zahari, *Polymers*, **15**, 1229 (2023), https//doi.org/10.3390/polym15051229

[5] I. Elfaleh, F. Abbassi, M. Habibi, F. Ahmad, M. Guedri *et al*., *Results Eng*., **19**, 101271 (2023), https://doi.org/10.1016/j.rineng.2023.101271

[6] A. Pokharel, K. J. Falua, A. Babaei-Ghazvini and B. Acharya, *J. Compos. Sci*., **6**, 255 (2022), https://doi.org/10.3390/jcs6090255

[7] M. J. Mochane, T. C. Mokhena, T. H. Mokhothu, A. Mtibe, E. R. Sadiku *et al*., *Express Polym. Lett.*, **13**, 159 (2019), https://doi.org/10.3144/expresspolymlett.2019.15
[8] M. Ö. Seydibeyoğlu, A. Dogru, J. Wang, M. Rencheck, Y. Han *et al*., *Polymers*, **15**, 984 (2023), https://doi.org/10.3390/polym15040984
[9] M. Shamsuyeva, O. Hansen and H. -J. Endres, *Int. J. Polym. Sci.*, **2019**, 1 (2019), https://doi.org/10.1155/2019/9624670
[10] M. Samanth, P. Hiremath, G. Divya Deepak, N. Naik, H. S. Arukumar *et al*., *J. Compos. Sci*., **9**, 124 (2025). https://doi.org/10.3390/jcs9030124
[11] C. J. Medina-Martinez, L. C. Sandoval Herazo, S. A. Zamora-Castro, R. Vivar-Ocampo and D. Reyes-Gonzalez, *Fibers*, **11**, 58 (2023), https://doi.org/10.3390/fib11070058
[12] D. Shelly, S. Lee and S. Park, *Adv. Compos. Hybrid Mater*., **8** (2025), https://doi.org/10.1007/s42114-025-01314-0
[13] M. Mariana, T. Alfatah, H. P. S. Abdul Khalil, E. B. Yahya, N. G. Laiya *et al*., *J. Mater. Res. Tech*., **15**, 2287 (2021), https://doi.org/10.1016/j.jmrt.2021.08.139
[14] S. T. Sikhosana, N. J. Malebo, M. P. Motloung, T. G. Mofokeng and M. J. Mochane, *Polymers*, **17**, 2120 (2025), https://doi.org/10.3390/polym17152120
[15] L. Theys, M. J. Mochane, T. G. Mofokeng, M. T. Motloung, M. P. Motloung *et al*., *J. Thermoplast. Compos. Mater*., **2025**, 1 (2025), https://doi.org/10.1177/08927057251329245
[16] D. Empty-Marin, L. M. Chiarello, V. R. Wiggers, A. Dantas and V. Botton, *Polimeros*, **33**, (2023)
[17] Y. Yang, Y. Chen, F. Leng, L. Huang, Z. Wang *et al*., *Appl. Sci*., **7**, 1215 (2017), https://doi.org/10.3390/app7121215
[18] Y. Hu, J. M. Zhang, H. Sato, I. Noda, Y. Ozaki *et al*., *Polymer*, **48**, 4777 (2007), https://doi.org/10.1016/j.polymer.2007.06.016
[19] B. Brugnoli, C. A. Lancia, A. Piozzi and I. Francolini, *J. Appl. Polym. Sci*., **142**, e57545 (2025), https://doi.org/10.1002/app.57545
[20] M. A. Masanabo, A. Tribot, E. Luoma, J. Virkajärvi, N. Sharmin *et al*., *Macromol. Mater. Eng*., **309**, 240037 (2024), https://doi.org/10.1002/mame.202400037
[21] B. F. A. Valente, A. J. D. Silvestre, C. P. Neto, C. Vilela and C. S. R. Freire, *Molecules*, **26**, 5594 (2021), https://doi.org/10.3390/molecules26185594
[22] J. Ivorra-Martinez, J. Manuel-Mañogil, T. Boronat, L. Sanchez-Nacher and R. Balart *et al*., *Polymers*, **12**, 1097 (2020), https://doi.org/10.3390/polym12051097
[23] L. Hilliou and J. Covas, *Polym. Int*., **70**, 24 (2020), https://doi.org/10.1002/pi.6093
[24] A. Pawlak and J. Krajenta, *Molecules*, **29**, 3410 (2024), https://doi.org/10.3390/molecules29143410
[25] D. Kun, Z. Kárpáti, E. Fekete and J. Móczó, *Polymers*, **13**, 3099 (2021), https://doi.org/10.3390/polym13183099
[26] K. Liu, S. Lai, J. Han and K. Hsieh, *Polym. Compos*., **41**, 4277 (2020), https://doi.org/10.1002/pc.25710